

Radiative transfer modeling of the enigmatic scattering polarization in the solar Na I D₁ line

LUCA BELLUZZI^{1,2}, JAVIER TRUJILLO BUENO^{3,4,5}, AND EGIDIO LANDI DEGL'INNOCENTI⁶

ABSTRACT

The modeling of the peculiar scattering polarization signals observed in some diagnostically important solar resonance lines requires the consideration of the detailed spectral structure of the incident radiation field as well as the possibility of ground level polarization, along with the atom's hyperfine structure and quantum interference between hyperfine F -levels pertaining either to the same fine structure J -level, or to different J -levels of the same term. Here we present a theoretical and numerical approach suitable for solving this complex non-LTE radiative transfer problem. This approach is based on the density-matrix metalevel theory (where each level is viewed as a continuous distribution of sublevels) and on accurate formal solvers of the transfer equations and efficient iterative methods. We show an application to the D-lines of Na I, with emphasis on the enigmatic D₁ line, pointing out the observable signatures of the various physical mechanisms considered. We demonstrate that the linear polarization observed in the core of the D₁ line may be explained by the effect that one gets when the detailed spectral structure of the anisotropic radiation responsible for the optical pumping is taken into account. This physical ingredient is capable of introducing significant scattering polarization in the core of the Na I D₁ line without the need for ground-level polarization.

Subject headings: atomic processes – line: formation – polarization – radiative transfer – scattering – stars: atmospheres

1. Introduction

For nearly two decades, the modeling of the scattering polarization signals observed by Stenflo & Keller (1997) in the core of the Na I and Ba II D₁ lines has represented one of the most challenging problems in the

¹Istituto Ricerche Solari Locarno, CH-6605 Locarno Monti, Switzerland

²Kiepenheuer-Institut für Sonnenphysik, D-79104 Freiburg, Germany

³Instituto de Astrofísica de Canarias, E-38205 La Laguna, Tenerife, Spain

⁴Departamento de Astrofísica, Facultad de Física, Universidad de La Laguna, E-38206 La Laguna, Tenerife, Spain

⁵Consejo Superior de Investigaciones Científicas, Spain

⁶Dipartimento di Fisica e Astronomia, Università di Firenze, I-50125 Firenze, Italy

field of theoretical spectropolarimetry (see also Stenflo et al. 2000). Given that these spectral lines are produced by atomic transitions between an upper level and a lower level with total angular momentum $J = 1/2$ (i.e., atomic levels that cannot carry atomic alignment), they were initially considered to be intrinsically unpolarizable lines. On the other hand, the only stable isotope of sodium (^{23}Na) and two of the seven stable isotopes of barium (^{135}Ba and ^{137}Ba , with relative abundances of about 7% and 11%, respectively) have nuclear spin $I = 3/2$. In these isotopes, the upper and lower levels of the D_1 line split into two hyperfine structure (HFS) levels with total (electronic plus nuclear) angular momenta $F = 1$ and $F = 2$. Therefore, the main problem is identifying a physical mechanism through which atomic alignment can be induced in the F -levels of the D_1 line.

According to the theory of spectral line polarization described in Landi Degl’Innocenti & Landolfi (2004), the mere absorption of anisotropic radiation is not sufficient to induce atomic alignment in the upper F -levels of the D_1 line, unless the lower F -levels are also polarized. As shown in Sect. 2 of Belluzzi & Trujillo Bueno (2013), this is ultimately due to the hypothesis, required by the theory of Landi Degl’Innocenti & Landolfi (2004), that the incident radiation field is flat (i.e., independent of frequency) across the spectral interval spanned by the HFS components of the D_1 line (flat-spectrum approximation). This assumption, on the other hand, does not appear to be particularly unsuitable in the solar case, since the frequency separation among the various HFS components of the D_1 line is significantly smaller than the Doppler width of the spectral line.

By generalizing the idea of “internal levels” (or “metalevels”) to the polarized case, Landi Degl’Innocenti et al. (1997) developed a theoretical approach that does not require the flat-spectrum condition to be satisfied, and that is suitable for treating coherent scattering processes in the presence of pumping radiation fields with an arbitrary spectral structure. Working within the framework of this theory, and assuming that the anisotropy degree of the incident radiation is constant with frequency, Landi Degl’Innocenti (1998, 1999) showed that a conspicuous polarization signal, similar to the observed one, can be produced in the core of the $\text{Na } D_1$ line, provided that a substantial amount of atomic polarization is present in the lower level (the ground level of sodium). This result, on the other hand, leads to a sort of paradox since the required atomic polarization in the long-lived ground level of sodium is incompatible with the presence in the lower solar chromosphere of inclined magnetic fields sensibly stronger than 0.01 G (see Landi Degl’Innocenti 1998), which seems to contradict the results obtained from other types of observations (e.g., Bianda et al. 1998; Stenflo et al. 1998). Moreover, through a calculation based on Quantum Chemistry, Kerkeni & Bommier (2002) argued that the effect of depolarizing collisions is sufficiently strong to destroy the required atomic polarization in the ground level of sodium.

In the work of Landi Degl’Innocenti (1998), lower level polarization was included in the problem as a free parameter. The physical mechanism through which atomic polarization can be induced in the ground level of sodium via the D_2 line transition, and then transferred to the upper F -levels of the D_1 line (the repopulation pumping mechanism), was pointed out by Trujillo Bueno et al. (2002), who in addition investigated the sensitivity of the atomic polarization of the sodium HFS levels to the presence of magnetic fields (see also Casini et al. 2002). These works, which were carried out within the framework of the theory of polarization described in Landi Degl’Innocenti & Landolfi (2004), neglecting depolarizing collisions,

showed the actual possibility of inducing a significant amount of atomic polarization in the ground level of sodium, but also confirmed its incompatibility with the estimated intensities and geometries of the magnetic fields of the lower chromosphere.

The “enigma” of the D_1 lines remained substantially unchanged until the recent identification by Belluzzi & Trujillo Bueno (2013) and by Del Pino Alemán et al. (2014) of two mechanisms that can introduce scattering polarization in the core of such lines, without requiring the presence of atomic polarization in the ground levels of sodium and barium. The idea at the basis of the mechanism identified by Belluzzi & Trujillo Bueno (2013) is that if the incident radiation field (and, in particular, its anisotropy degree) varies across the HFS multiplet, so that the various HFS components are affected by different pumping radiations, then atomic polarization can be induced in the upper F -levels of the D_1 line, and the emitted radiation can in general be polarized, also in the absence of atomic polarization in the lower F -levels. Belluzzi & Trujillo Bueno (2013) modeled the D_1 lines of Na I and Ba II by solving the full non-LTE radiative transfer (RT) problem in one-dimensional semi-empirical models of the solar atmosphere, according to the partial frequency redistribution (PRD) approach described in Belluzzi & Trujillo Bueno (2014). Through the R_{II} part of their redistribution matrix, which describes coherent scattering processes according to the metalevel approach, they took into account the detailed spectral structure of the pumping radiation, finding that the small differences among the radiation fields experienced by the various HFS components of the D_1 line are actually sufficient to produce appreciable scattering polarization signals in the core of these lines.

The signal obtained by Belluzzi & Trujillo Bueno (2013) in the core of the Na I D_1 line is, however, sensibly weaker than the one observed by Stenflo & Keller (1997), but it is similar to that shown in the right panel of Figure 2 of Trujillo Bueno (2009), resulting from the observations by Trujillo Bueno et al. (2001). On the other hand, two physical ingredients, which were taken into account by Landi Degl’Innocenti (1998), have been neglected by Belluzzi & Trujillo Bueno (2013): quantum interference between HFS magnetic sublevels pertaining to different J -levels, and the possibility that a given amount of atomic polarization is present in the lower F -levels. It is well known that interference between the upper J -levels of the D_1 and D_2 lines plays a very important role in the generation of the scattering polarization pattern observed in these lines (see Stenflo 1980; Landi Degl’Innocenti 1998; Landi Degl’Innocenti & Landolfi 2004), while recent RT calculations seem to indicate that in the atmospheric region where the core of the sodium D-lines is formed depolarizing collisions might not completely destroy lower level polarization as previously thought.

In the first part of this paper, we derive a redistribution matrix suitable for describing coherent scattering in the atom rest frame (with Doppler redistribution in the observer’s frame), accounting for lower level polarization, interference between HFS magnetic sublevels pertaining to the upper J -levels of D_1 and D_2 , and inelastic collisions with electrons. In the second part, we describe the numerical method of solution of the ensuing non-LTE problem, and we present a series of results obtained by treating lower level polarization as a free parameter of the problem (it will not be calculated self-consistently when solving the non-LTE problem).

As previously mentioned, another mechanism that may explain the physical origin of the signals ob-

served by Stenflo & Keller (1997) and Stenflo et al. (2000) in the core of the Na I and Ba II D₁ lines, without requiring the presence of lower level polarization, has been recently identified by Del Pino Alemán et al. (2014). In their work, the authors show that measurable Q/I signals can be produced in the core of intrinsically unpolarizable lines through the redistribution of the spectral line radiation due to the non-coherence of the continuum scattering. Although this mechanism (which strongly depends on the assumed model atmosphere) may well coexist with the previous one, it will be neglected in this investigation.

Finally, we point out that the enigmatic polarization signals observed in the solar D₁ line have led to the realization of a laboratory experiment on scattering polarization by the potassium atom, which has the same D₁ quantum structure as sodium (Thalmann et al. 2006, 2009). This experiment, performed by pumping the potassium atoms through a tunable laser, has shown an unexpected phenomenology that cannot be interpreted by means of the standard Kramers-Heisenberg equation. Stenflo (2015) has recently suggested an interpretation of these results based on quantum interference between the sublevels of the ground state of potassium. It will be of interest to investigate whether this physical ingredient may also play a role in the solar case, but this lies outside the scope of the present paper. This kind of interference is thus neglected in the present work.

2. Formulation of the problem

We consider a two-term atom with HFS, in the absence of magnetic fields. Under the assumption of L - S coupling, the atomic Hamiltonian has eigenvectors of the form $|\beta L S I J F M\rangle$, where β , L , and S indicate the electronic configuration, the orbital angular momentum, and the electronic spin, respectively, I is the nuclear spin, J the total electronic angular momentum, F the total (electronic plus nuclear) angular momentum, and M its projection along the quantization axis. We recall that each term is composed of $(L + S - |L - S| + 1)$ fine structure (FS) J -levels, while each J -level splits into $(J + I - |J - I| + 1)$ HFS F -levels. In each term, we thus have

$$\sum_{J=|L-S|}^{L+S} \left(\sum_{F=|J-I|}^{J+I} (2F+1) \right) = (2L+1)(2S+1)(2I+1), \quad (1)$$

magnetic sublevels.

In the standard representation, the atomic model under consideration is described by the density matrix elements

$${}^{\beta L S I} \rho(J F M, J' F' M') \equiv \langle \beta L S I J F M | \hat{\rho} | \beta L S I J' F' M' \rangle, \quad (2)$$

with $\hat{\rho}$ the density operator. As is clear from Eq. (2), this atomic model accounts for quantum interference between pairs of HFS magnetic sublevels belonging either to the same F -level or to different F -levels pertaining either to the same J -level or to different J -levels within the same term. In the following, we will work with the irreducible spherical components of the density matrix (or spherical statistical tensors) defined by (see Eq. (11b) of Casini & Manso Sainz 2005)

$${}^{\beta L S I} \rho_Q^K(J F, J' F') = \sum_{M M'} (-1)^{F-M} \sqrt{2K+1} \begin{pmatrix} F & F' & K \\ M & -M' & -Q \end{pmatrix} {}^{\beta L S I} \rho(J F M, J' F' M'). \quad (3)$$

Equation (3) shows that in a two-term (or multi-term) atom with HFS, besides the 0-rank elements ${}^{\beta L S I} \rho_0^0(JF, JF)$, which are proportional to the population of a given HFS level, we also have non-diagonal 0-rank elements of the form ${}^{\beta L S I} \rho_0^0(JF, J'F)$, which describe interference between pairs of magnetic sublevels with the same M and F quantum numbers, but pertaining to different J -levels.

We take lower term polarization into account, but only in the form of population imbalances among the various magnetic sublevels of the same F -level (interference between pairs of magnetic sublevels pertaining either to the same F -level or to different F -levels of the lower term is instead neglected by definition).¹ Within the framework of the density matrix formalism, this hypothesis reads

$${}^{\beta_\ell L_\ell S I} \rho_Q^K(J_\ell F_\ell, J'_\ell F'_\ell) = \delta_{J_\ell J'_\ell} \delta_{F_\ell F'_\ell} \delta_{Q0} {}^{\beta_\ell L_\ell S I} \rho_0^K(J_\ell F_\ell, J_\ell F_\ell), \quad (4)$$

where the label ℓ indicates that the corresponding quantity refers to the lower term, or to one of its FS or HFS levels (accordingly, quantities of the upper term will be labeled with the letter u). Furthermore, we assume that the populations of the various HFS F -levels of the lower term, $\mathcal{N}(J_\ell, F_\ell)$, are proportional to the statistical weights:

$$\mathcal{N}(J_\ell, F_\ell) = \frac{\mathcal{N}(L_\ell)}{(2L_\ell + 1)(2S + 1)(2I + 1)} (2F_\ell + 1), \quad (5)$$

with $\mathcal{N}(L_\ell)$ the overall population of the lower term. Indicating with \mathcal{N}_T the total population, we have

$${}^{\beta_\ell L_\ell S I} \rho_0^0(J_\ell F_\ell, J_\ell F_\ell) = \frac{1}{\mathcal{N}_T} \frac{\mathcal{N}(J_\ell, F_\ell)}{\sqrt{2F_\ell + 1}} = \frac{\mathcal{N}(L_\ell)}{\mathcal{N}_T} \frac{\sqrt{2F_\ell + 1}}{(2L_\ell + 1)(2S + 1)(2I + 1)}. \quad (6)$$

Introducing the quantity

$$\sigma_0^K(J_\ell, F_\ell) = \frac{{}^{\beta_\ell L_\ell S I} \rho_0^K(J_\ell F_\ell, J_\ell F_\ell)}{{}^{\beta_\ell L_\ell S I} \rho_0^0(J_\ell F_\ell, J_\ell F_\ell)}, \quad (7)$$

we can finally write

$${}^{\beta_\ell L_\ell S I} \rho_Q^K(J_\ell F_\ell, J'_\ell F'_\ell) = \delta_{J_\ell J'_\ell} \delta_{F_\ell F'_\ell} \delta_{Q0} \frac{\mathcal{N}(L_\ell)}{\mathcal{N}_T} \frac{\sqrt{2F_\ell + 1}}{(2L_\ell + 1)(2S + 1)(2I + 1)} \sigma_0^K(J_\ell, F_\ell). \quad (8)$$

In this work, the quantity $\sigma_0^K(J_\ell, F_\ell)$ is not calculated through a self-consistent solution of the statistical equilibrium equations and of the RT equations, but it is set as a free parameter of the problem.

We account for inelastic collisions with electrons, inducing transitions between the upper and the lower term. On the other hand, we neglect “weakly inelastic” collisions inducing transitions between different FS or HFS levels pertaining to the same term, as well as elastic collisions with neutral perturbers. Finally, we assume that the magnetic sublevels of the lower term are infinitely sharp. In the atom rest frame, this last set of hypotheses implies coherence in frequency for Rayleigh scattering, and the usual energy conservation relationship between the frequencies of the incoming and outgoing photons for Raman scattering. Stimulated emission is neglected.

¹Note that in the recent modeling of polarized scattering by tunable laser light on potassium gas in the laboratory, quantum coherence in the lower term was identified as the source of the observed D_1 polarization (Stenflo 2015). It will be of interest to investigate whether this coherence may play a significant role also in the solar case, where the pumping radiation is broadband and not nearly monochromatic and highly polarized (as in a tunable laser). In this work, we demonstrate that it is possible to obtain significant solar D_1 polarization by neglecting them.

3. The absorption and emission coefficients

The expression of the absorption coefficient for a two-term atom with HFS, accounting for lower term polarization and for the presence of an arbitrary magnetic field, is given by Eq. (33a) of Casini & Manso Sainz (2005). With the help of Eq. (2.34) of Landi Degl’Innocenti & Landolfi (2004), it can be shown that in the absence of magnetic fields, it takes the simpler form

$$\begin{aligned} \eta_i(\nu, \vec{\Omega}) = & \frac{h\nu}{4\pi} \mathcal{N}_T(2L_\ell + 1) B(L_\ell \rightarrow L_u) \sum_{KQ} \sum_{J_\ell F_\ell} \sum_{J'_\ell F'_\ell} \sum_{J_u F_u} (-1)^{1+K+J'_\ell-J_\ell-F_\ell-F_u} \\ & \times (2J_u + 1)(2F_u + 1) \sqrt{3(2J_\ell + 1)(2J'_\ell + 1)(2F_\ell + 1)(2F'_\ell + 1)} \\ & \times \left\{ \begin{matrix} J_u & J_\ell & 1 \\ F_\ell & F_u & I \end{matrix} \right\} \left\{ \begin{matrix} J_u & J'_\ell & 1 \\ F'_\ell & F_u & I \end{matrix} \right\} \left\{ \begin{matrix} L_u & L_\ell & 1 \\ J_\ell & J_u & S \end{matrix} \right\} \left\{ \begin{matrix} L_u & L_\ell & 1 \\ J'_\ell & J_u & S \end{matrix} \right\} \left\{ \begin{matrix} 1 & 1 & K \\ F_\ell & F'_\ell & F_u \end{matrix} \right\} \\ & \times \text{Re} \left\{ \mathcal{T}_Q^K(i, \vec{\Omega})^{\beta_\ell L_\ell S I} \rho_Q^K(J_\ell F_\ell, J'_\ell F'_\ell) \Phi(\nu_{J_u F_u, J_\ell F_\ell} - \nu) \right\}, \end{aligned} \quad (9)$$

with $i = 0, 1, 2, 3$, standing for Stokes I, Q, U , and V , respectively, and where $B(L_\ell \rightarrow L_u)$ is the Einstein coefficient for absorption from the lower to the upper term and $\mathcal{T}_Q^K(i, \vec{\Omega})$ is the geometrical tensor introduced by Landi Degl’Innocenti (1983). The complex profile $\Phi(\nu_0 - \nu)$ is defined by

$$\Phi(\nu_0 - \nu) = \phi(\nu_0 - \nu) + i\psi(\nu_0 - \nu), \quad (10)$$

with $\phi(\nu_0 - \nu)$ the Lorentzian profile and $\psi(\nu_0 - \nu)$ the associated dispersion profile.

Assuming that no interference is present in the lower term, so that the spherical statistical tensors of this term are given by Eq. (4), then Eq. (2) of Landi Degl’Innocenti (1999) is easily recovered. Substituting Eq. (8) into Eq. (9), we have

$$\eta_i(\nu, \vec{\Omega}) = k_L \sum_K \mathcal{T}_0^K(i, \vec{\Omega}) \alpha_0^K(\nu), \quad (11)$$

with

$$\begin{aligned} \alpha_0^K(\nu) = & \frac{1}{(2S + 1)(2I + 1)} \sum_{J_\ell F_\ell} \sum_{J_u F_u} (-1)^{1+K-F_\ell-F_u} \sqrt{3} (2J_u + 1)(2J_\ell + 1)(2F_u + 1)(2F_\ell + 1)^{3/2} \\ & \times \left\{ \begin{matrix} J_u & J_\ell & 1 \\ F_\ell & F_u & I \end{matrix} \right\}^2 \left\{ \begin{matrix} L_u & L_\ell & 1 \\ J_\ell & J_u & S \end{matrix} \right\}^2 \left\{ \begin{matrix} 1 & 1 & K \\ F_\ell & F_\ell & F_u \end{matrix} \right\} \sigma_0^K(J_\ell, F_\ell) \phi(\nu_{J_u F_u, J_\ell F_\ell} - \nu), \end{aligned} \quad (12)$$

and where we have introduced the frequency-integrated absorption coefficient

$$k_L = \frac{h\nu}{4\pi} \mathcal{N}(L_\ell) B(L_\ell \rightarrow L_u). \quad (13)$$

The expression of the emission coefficient for a two-term atom with HFS, in the absence of magnetic fields, neglecting any kind of collisions, assuming that no interference is present in the lower term, and under the assumption that the magnetic sublevels of the lower term are infinitely sharp, has been derived by Landi Degl’Innocenti (1999), working within the framework of the metalevel approach of Landi Degl’Innocenti et al.

(1997). This expression, which is given by Eq. (1) of Landi Degl’Innocenti (1999), can be rewritten in the equivalent form

$$\begin{aligned}
\varepsilon_i(\nu, \vec{\Omega}) = & \frac{h\nu}{4\pi} \mathcal{N}_T B(L_\ell \rightarrow L_u) (2L_u + 1)(2L_\ell + 1) \\
& \times \sum_{J_\ell J'_\ell} \sum_{J_u J'_u} \sum_{F_\ell F'_\ell} \sum_{F_u F'_u} \sum_{KQ} \sum_{K_r Q_r} \sum_{K_\ell} (-1)^{1+K_\ell+F_\ell+F_u} 3 \sqrt{(2K+1)(2K_r+1)(2K_\ell+1)} \\
& \times (2J_u+1)(2J'_u+1)(2J_\ell+1)(2J'_\ell+1)(2F_u+1)(2F'_u+1)(2F_\ell+1)(2F'_\ell+1) \\
& \times \begin{Bmatrix} L_u & L_\ell & 1 \\ J_\ell & J_u & S \end{Bmatrix} \begin{Bmatrix} L_u & L_\ell & 1 \\ J_\ell & J'_u & S \end{Bmatrix} \begin{Bmatrix} L_u & L_\ell & 1 \\ J'_\ell & J_u & S \end{Bmatrix} \begin{Bmatrix} L_u & L_\ell & 1 \\ J'_\ell & J'_u & S \end{Bmatrix} \\
& \times \begin{Bmatrix} J_u & J_\ell & 1 \\ F_\ell & F_u & I \end{Bmatrix} \begin{Bmatrix} J'_u & J_\ell & 1 \\ F_\ell & F'_u & I \end{Bmatrix} \begin{Bmatrix} J_u & J'_\ell & 1 \\ F'_\ell & F_u & I \end{Bmatrix} \begin{Bmatrix} J'_u & J'_\ell & 1 \\ F'_\ell & F'_u & I \end{Bmatrix} \\
& \times \begin{Bmatrix} K & F_u & F'_u \\ F_\ell & 1 & 1 \end{Bmatrix} \begin{Bmatrix} K & K_r & K_\ell \\ F'_u & 1 & F'_\ell \\ F_u & 1 & F'_\ell \end{Bmatrix} \begin{pmatrix} K & K_r & K_\ell \\ -Q & -Q_r & 0 \end{pmatrix} \\
& \times \mathcal{T}_Q^K(i, \vec{\Omega}) J_{Q_r}^{K_r}(\nu - \nu_{J'_\ell F'_\ell, J_\ell F_\ell})^{\beta_\ell L_\ell S I} \rho_0^{K_\ell}(J'_\ell F'_\ell, J'_\ell F'_\ell) \frac{1}{2} \left[\frac{\Phi(\nu_{J_u F_u, J_\ell F_\ell} - \nu) + \Phi(\nu_{J'_u F'_u, J_\ell F_\ell} - \nu)^*}{1 + 2\pi i \nu_{J'_u F'_u, J_u F_u} / A(L_u \rightarrow L_\ell)} \right], \tag{14}
\end{aligned}$$

where $A(L_u \rightarrow L_\ell)$ is the Einstein coefficient for spontaneous emission from the upper to the lower term, while ν_{ab} is the frequency separation between levels a and b . The tensor $J_{Q_r}^{K_r}(\nu')$ describing the incident radiation field is given by (see Eq. (5.157) of Landi Degl’Innocenti & Landolfi 2004)

$$J_{Q_r}^{K_r}(\nu') = \oint \frac{d\Omega'}{4\pi} \sum_{j=0}^3 \mathcal{T}_{Q_r}^{K_r}(j, \vec{\Omega}') I_j(\nu', \vec{\Omega}'), \tag{15}$$

with $I_j(\nu', \vec{\Omega}')$ the four Stokes parameters.

In order to take the effect of inelastic collisions with electrons into account, we proceed by analogy with the complete frequency redistribution (CRD) case. The expression of the emission coefficient for a two-term atom with HFS, in the limit of CRD, taking such collisions into account, has been derived by Belluzzi et al. (2015), working within the framework of the theory of Landi Degl’Innocenti & Landolfi (2004). By analogy with Eq. (37) of Belluzzi et al. (2015), we thus include the effect of inelastic collisions by modifying Eq. (14) as follows

$$\begin{aligned}
\varepsilon_i(\nu, \vec{\Omega}) = & \frac{h\nu}{4\pi} \mathcal{N}_T B(L_\ell \rightarrow L_u) (2L_u + 1)(2L_\ell + 1) \\
& \times \sum_{J_\ell J'_\ell} \sum_{J_u J'_u} \sum_{F_\ell F'_\ell} \sum_{F_u F'_u} \Upsilon(L_u L_\ell S I, J_u J'_u J_\ell J'_\ell F_u F'_u F_\ell F'_\ell) \frac{1}{2} \left[\frac{\Phi(\nu_{J_u F_u, J_\ell F_\ell} - \nu) + \Phi(\nu_{J'_u F'_u, J_\ell F_\ell} - \nu)^*}{1 + \epsilon' + 2\pi i \nu_{J'_u F'_u, J_u F_u} / A(L_u \rightarrow L_\ell)} \right] \\
& \times \sum_{KQ} \sum_{K_r Q_r} \sum_{K_\ell} (-1)^{1+K_\ell+F_\ell+F_u} 3 \sqrt{(2K+1)(2K_r+1)(2K_\ell+1)}
\end{aligned}$$

$$\begin{aligned}
& \times \left\{ \begin{array}{ccc} K & F_u & F'_u \\ F_\ell & 1 & 1 \end{array} \right\} \left\{ \begin{array}{ccc} K & K_r & K_\ell \\ F'_u & 1 & F'_\ell \\ F_u & 1 & F_\ell \end{array} \right\} \left\{ \begin{array}{ccc} K & K_r & K_\ell \\ -Q & -Q_r & 0 \end{array} \right\} \\
& \times \mathcal{T}_Q^K(i, \vec{\Omega}) J_{Q_r}^{K_r} (\nu - \nu_{J'_\ell F'_\ell, J_\ell F_\ell})^{\beta_\ell L_\ell S I} \rho_0^{K_\ell} (J'_\ell F'_\ell, J'_\ell F'_\ell) + \varepsilon_i^{\text{coll}}(\nu, \vec{\Omega}), \tag{16}
\end{aligned}$$

where, in order to simplify the notation, we have introduced the quantity

$$\begin{aligned}
\Upsilon(L_u L_\ell S I, J_u J'_u J_\ell J'_\ell F_u F'_u F_\ell F'_\ell) &= (2J_u + 1)(2J'_u + 1)(2J_\ell + 1)(2J'_\ell + 1)(2F_u + 1)(2F'_u + 1)(2F_\ell + 1)(2F'_\ell + 1) \\
&\times \left\{ \begin{array}{ccc} L_u & L_\ell & 1 \\ J_\ell & J_u & S \end{array} \right\} \left\{ \begin{array}{ccc} L_u & L_\ell & 1 \\ J_\ell & J'_u & S \end{array} \right\} \left\{ \begin{array}{ccc} L_u & L_\ell & 1 \\ J'_\ell & J_u & S \end{array} \right\} \left\{ \begin{array}{ccc} L_u & L_\ell & 1 \\ J'_\ell & J'_u & S \end{array} \right\} \\
&\times \left\{ \begin{array}{ccc} J_u & J_\ell & 1 \\ F_\ell & F_u & I \end{array} \right\} \left\{ \begin{array}{ccc} J'_u & J_\ell & 1 \\ F_\ell & F'_u & I \end{array} \right\} \left\{ \begin{array}{ccc} J_u & J'_\ell & 1 \\ F'_\ell & F_u & I \end{array} \right\} \left\{ \begin{array}{ccc} J'_u & J'_\ell & 1 \\ F'_\ell & F'_u & I \end{array} \right\}. \tag{17}
\end{aligned}$$

As in the CRD case, the quantity ϵ' is defined by

$$\epsilon' = \frac{C_S(L_u \rightarrow L_\ell)}{A(L_u \rightarrow L_\ell)}, \tag{18}$$

where $C_S(L_u \rightarrow L_\ell)$ is the inelastic collision rate for the transition from the upper to the lower term (see Eq. (21) of Belluzzi et al. 2015, and the discussion therein). The term $\varepsilon_i^{\text{coll}}(\nu, \vec{\Omega})$, which represents the contribution to the emission coefficient brought by collisionally excited atoms, is given by (see Eq. (37) of Belluzzi et al. 2015)

$$\begin{aligned}
\varepsilon_i^{\text{coll}}(\nu, \vec{\Omega}) &= \frac{h\nu}{4\pi} \mathcal{N}_T B(L_\ell \rightarrow L_u) (2L_u + 1)(2L_\ell + 1) \epsilon' B_T(\nu_0) \\
&\times \sum_{J_\ell J'_\ell} \sum_{J_u J'_u} \sum_{F_\ell F'_\ell} \sum_{F_u F'_u} \Upsilon(L_u L_\ell S I, J_u J'_u J_\ell J'_\ell F_u F'_u F_\ell F'_\ell) \frac{1}{2} \left[\frac{\Phi(\nu_{J_u F_u, J_\ell F_\ell} - \nu) + \Phi(\nu_{J'_u F'_u, J'_\ell F'_\ell} - \nu)^*}{1 + \epsilon' + 2\pi i \nu_{J'_u F'_u, J_u F_u} / A(L_u \rightarrow L_\ell)} \right] \\
&\times \sum_K (-1)^{F_u - F'_u - F_\ell + F'_\ell + K} \sqrt{3} \left\{ \begin{array}{ccc} K & F_u & F'_u \\ F_\ell & 1 & 1 \end{array} \right\} \left\{ \begin{array}{ccc} F'_u & F'_\ell & 1 \\ F'_\ell & F_u & K \end{array} \right\} \mathcal{T}_0^K(i, \vec{\Omega})^{\beta_\ell L_\ell S I} \rho_0^K(J'_\ell F'_\ell, J'_\ell F'_\ell), \tag{19}
\end{aligned}$$

where $B_T(\nu_0)$ is the Planck function in the Wien limit (consistently with our assumption of neglecting stimulated emission), at the frequency $\nu_0 = (E(L_u) - E(L_\ell))/h$, with $E(L_u)$ and $E(L_\ell)$ the energies of the centers of gravity of the upper and lower term, respectively, and h the Planck constant.

4. The R_{II} redistribution matrix

Recalling the definition of the radiation field tensor (see Eq. (15)), the emission coefficient of Eq. (16) can be expressed in terms of a suitable redistribution matrix (R_{II} following the terminology introduced by

Hummer 1962). Following the convention according to which unprimed quantities refer to the scattered radiation while primed quantities refer to the incident radiation, we can write

$$\varepsilon_i(\nu, \vec{\Omega}) = \int d\nu' \int \frac{d\Omega'}{4\pi} \sum_{j=0}^3 [R_{II}(\nu', \vec{\Omega}'; \nu, \vec{\Omega})]_{ij} I_j(\nu', \vec{\Omega}') + \varepsilon_i^{\text{coll.}}(\nu, \vec{\Omega}), \quad (20)$$

with

$$\begin{aligned} [R_{II}(\nu', \vec{\Omega}'; \nu, \vec{\Omega})]_{ij} &= \frac{h\nu}{4\pi} \mathcal{N}_T B(L_\ell \rightarrow L_u) (2L_u + 1)(2L_\ell + 1) \\ &\times \sum_{J_\ell J'_\ell} \sum_{J_u J'_u} \sum_{F_\ell F'_\ell} \sum_{F_u F'_u} \Upsilon(L_u L_\ell S I, J_u J'_u J_\ell J'_\ell F_u F'_u F_\ell F'_\ell) \\ &\times \frac{1}{2} \left[\frac{\Phi(\nu_{J_u F_u, J_\ell F_\ell} - \nu) + \Phi(\nu_{J'_u F'_u, J'_\ell F'_\ell} - \nu)^*}{1 + \epsilon' + 2\pi i \nu_{J'_u F'_u, J_u F_u} / A(L_u \rightarrow L_\ell)} \right] \delta(\nu - \nu' - \nu_{J'_\ell F'_\ell, J_\ell F_\ell}) \\ &\times \sum_{KQ} \sum_{K_r Q_r} \sum_{K_\ell} (-1)^{1+K_\ell+F_u+F_\ell} 3 \sqrt{(2K+1)(2K_r+1)(2K_\ell+1)} \\ &\times \begin{Bmatrix} K & F_u & F'_u \\ F_\ell & 1 & 1 \end{Bmatrix} \begin{pmatrix} K & K_r & K_\ell \\ -Q & -Q_r & 0 \end{pmatrix} \begin{Bmatrix} K & K_r & K_\ell \\ F'_u & 1 & F'_\ell \\ F_u & 1 & F_\ell \end{Bmatrix} \\ &\times \mathcal{T}_Q^K(i, \vec{\Omega}) \mathcal{T}_{Q_r}^{K_r}(j, \vec{\Omega}') \beta_{\ell L_\ell S I}^{\beta_{\ell L_\ell S I}} \rho_0^{K_\ell}(J'_\ell F'_\ell, J_\ell F_\ell). \end{aligned} \quad (21)$$

The R_{II} redistribution matrix derived above is valid in the atom rest frame. In order to find the corresponding expression in the observer's frame, one has to take the Doppler effect into account for the given velocity distribution of the atoms. The derivation is similar to that outlined in Belluzzi & Trujillo Bueno (2014) and will not be given here. Assuming that the atoms have a Maxwellian distribution of velocities, characterized by the temperature T , it can be demonstrated that the expression of the R_{II} redistribution matrix in the observer's frame is obtained by performing the following substitution in Eq. (21)

$$\begin{aligned} \frac{1}{2} \left[\frac{\Phi(\nu_{J_u F_u, J_\ell F_\ell} - \nu) + \Phi(\nu_{J'_u F'_u, J'_\ell F'_\ell} - \nu)^*}{1 + \epsilon' + 2\pi i \nu_{J'_u F'_u, J_u F_u} / A(L_u \rightarrow L_\ell)} \right] \delta(\nu - \nu' - \nu_{J'_\ell F'_\ell, J_\ell F_\ell}) \rightarrow \\ \frac{1}{1 + \epsilon' + 2\pi i \nu_{J'_u F'_u, J_u F_u} / A(L_u \rightarrow L_\ell)} \frac{1}{\pi \Delta \nu_D^2 \sin \theta} \exp \left[- \left(\frac{\nu' - \nu - \nu_{J'_\ell F'_\ell, J_\ell F_\ell}}{2 \Delta \nu_D \sin \theta / 2} \right)^2 \right] \\ \times \frac{1}{2} \left[W \left(\frac{a}{\cos \theta / 2}, \frac{x_{J_u F_u, J_\ell F_\ell} + x'_{J'_u F'_u, J'_\ell F'_\ell}}{2 \cos \theta / 2} \right) + W \left(\frac{a}{\cos \theta / 2}, \frac{x_{J'_u F'_u, J_\ell F_\ell} + x'_{J_u F_u, J'_\ell F'_\ell}}{2 \cos \theta / 2} \right)^* \right], \end{aligned} \quad (22)$$

where $\Delta \nu_D$ is the Doppler width in frequency units, and θ the scattering angle. The complex profile $W(\alpha, \beta)$ is defined as

$$W(\alpha, \beta) = H(\alpha, \beta) + iL(\alpha, \beta), \quad (23)$$

with H and L the Voigt and Faraday-Voigt functions, respectively. The damping parameter a is given by

$$a = \frac{\Gamma}{4\pi \Delta \nu_D}, \quad (24)$$

with Γ the broadening constant of the upper level (we recall that the lower level is assumed to be infinitely sharp). We assume that the various HFS levels of the upper term are characterized by the same broadening constant. In the applications shown in Sect. 7, Γ is calculated including the contributions due to radiative and collisional decays from the upper to the lower term, and the contribution of elastic collisions²

$$\Gamma = \Gamma_R + \Gamma_I + \Gamma_E = A(L_u \rightarrow L_\ell) + C_S(L_u \rightarrow L_\ell) + Q_{\text{el}} , \quad (25)$$

with Q_{el} the rate of elastic collisions. The reduced frequencies x_{ab} and x'_{ab} are given by

$$x_{ab} = \frac{\nu_{ab} - \nu}{\Delta\nu_D} , \quad \text{and} \quad x'_{ab} = \frac{\nu_{ab} - \nu'}{\Delta\nu_D} . \quad (26)$$

In the observer's frame, the collisional term $\varepsilon_i^{\text{coll.}}(\nu, \vec{\Omega})$ and the absorption coefficient $\eta_i(\nu, \vec{\Omega})$ are still given by Eqs. (19) and (11), respectively, with the only difference being that the Lorentzian and the associated dispersion profiles entering the definition of the complex profile $\Phi(\nu_0 - \nu)$ (see Eq. (10)) are now the Voigt and the Faraday-Voigt profiles, respectively.

The numerical calculation of the R_{II} redistribution matrix of Eq. (21) is rather demanding since the angular and frequency dependencies cannot be factorized as in the atom rest frame. For this reason, it is customary to work with an approximate expression, obtained by averaging the frequency-dependent terms of the redistribution matrix over all the possible propagation directions $\vec{\Omega}'$ and $\vec{\Omega}$ of the incoming and outgoing photons (see Rees & Saliba 1982). Observing that this average can be easily reduced to an integral over the scattering angle θ , the “angle-averaged” observer's frame expression of the redistribution matrix is obtained by performing the following substitution in Eq. (21)

$$\begin{aligned} & \frac{1}{2} \left[\frac{\Phi(\nu_{J_u F_u, J_\ell F_\ell} - \nu) + \Phi(\nu_{J'_u F'_u, J_\ell F_\ell} - \nu)^*}{1 + \epsilon' + 2\pi i \nu_{J'_u F'_u, J_u F_u} / A(L_u \rightarrow L_\ell)} \right] \delta(\nu - \nu' - \nu_{J'_\ell F'_\ell, J_\ell F_\ell}) \rightarrow \\ & \frac{1}{1 + \epsilon' + 2\pi i \nu_{J'_u F'_u, J_u F_u} / A(L_u \rightarrow L_\ell)} \frac{1}{2\pi \Delta\nu_D^2} \int_0^\pi d\theta \exp \left[- \left(\frac{\nu' - \nu - \nu_{J'_\ell F'_\ell, J_\ell F_\ell}}{2 \Delta\nu_D \sin \theta/2} \right)^2 \right] \\ & \times \frac{1}{2} \left[W \left(\frac{a}{\cos \theta/2}, \frac{x_{J_u F_u, J_\ell F_\ell} + x'_{J'_u F'_u, J'_\ell F'_\ell}}{2 \cos \theta/2} \right) + W \left(\frac{a}{\cos \theta/2}, \frac{x_{J'_u F'_u, J_\ell F_\ell} + x'_{J_u F_u, J'_\ell F'_\ell}}{2 \cos \theta/2} \right)^* \right] . \quad (27) \end{aligned}$$

Using Eq. (8), we obtain the following final expression of the angle-averaged redistribution matrix

$$\left[R_{II-AA}(\nu', \vec{\Omega}'; \nu, \vec{\Omega}) \right]_{ij} = k_L \sum_{KQ} \mathcal{T}_Q^K(i, \vec{\Omega}) \sum_{K_r Q_r} \mathcal{T}_{Q_r}^{K_r}(j, \vec{\Omega}') r_{II-AA}(KQ, K_r Q_r; \nu', \nu) , \quad (28)$$

with

$$r_{II-AA}(KQ, K_r Q_r; \nu', \nu) = \frac{(2L_u + 1)}{(2S + 1)(2I + 1)} \sum_{J_\ell J'_\ell} \sum_{J_u J'_u} \sum_{F_\ell F'_\ell} \sum_{F_u F'_u} \sqrt{2F'_\ell + 1} \Upsilon(L_u L_\ell S I, J_u J'_u J_\ell J'_\ell F_u F'_u F_\ell F'_\ell)$$

² We recall that elastic collisions play three different, although intimately related, roles: they contribute to the broadening of the spectral lines, they redistribute the photon frequency during the scattering process, and they relax atomic polarization. In this work, we heuristically take the first effect into account through the damping parameter a , but we neglect the second and third ones.

$$\begin{aligned}
& \times \frac{1}{1 + \epsilon' + 2\pi i \nu J_u' F_u' / A(L_u \rightarrow L_\ell)} \frac{1}{2\pi \Delta \nu_D^2} \int_0^\pi d\theta \left\{ \exp \left[- \left(\frac{\nu' - \nu - \nu J_\ell' F_\ell' / A(L_\ell \rightarrow L_u)}{2 \Delta \nu_D \sin \theta / 2} \right)^2 \right] \right. \\
& \times \frac{1}{2} \left[W \left(\frac{a}{\cos \theta / 2}, \frac{x_{J_u F_u, J_\ell F_\ell} + x_{J_u F_u, J_\ell' F_\ell'}}{2 \cos \theta / 2} \right) + W \left(\frac{a}{\cos \theta / 2}, \frac{x_{J_u' F_u', J_\ell F_\ell} + x_{J_u' F_u', J_\ell' F_\ell'}}{2 \cos \theta / 2} \right)^* \right] \Bigg\} \\
& \times \sum_{K_\ell} (-1)^{1+K_\ell+F_u+F_\ell} 3 \sqrt{(2K+1)(2K_r+1)(2K_\ell+1)} \\
& \times \begin{Bmatrix} K & F_u & F_u' \\ F_\ell & 1 & 1 \end{Bmatrix} \begin{Bmatrix} K & K_r & K_\ell \\ -Q & -Q_r & 0 \end{Bmatrix} \begin{Bmatrix} K & K_r & K_\ell \\ F_u' & 1 & F_\ell' \\ F_u & 1 & F_\ell' \end{Bmatrix} \sigma_0^{K_\ell}(J_\ell', F_\ell'). \quad (29)
\end{aligned}$$

As a consistency check, we verified that neglecting lower term polarization (i.e., setting $\sigma_0^{K_\ell}(J_\ell', F_\ell') = \delta_{K_\ell 0}$), and in the absence of HFS (i.e., setting $I = 0$), Eq. (28) reduces to Eq. (35) of Belluzzi & Trujillo Bueno (2014). Likewise, substituting Eq. (8) into Eq. (19), the collisional term can be written in the form

$$\mathcal{E}_i^{\text{coll.}}(\nu, \vec{\Omega}) = k_L \sum_K \mathcal{T}_0^K(i, \vec{\Omega}) B_T(\nu_0) \beta_0^K(\nu), \quad (30)$$

with

$$\begin{aligned}
\beta_0^K(\nu) &= \frac{(2L_u + 1)}{(2S + 1)(2I + 1)} \sum_{J_\ell' J_\ell} \sum_{J_u' J_u} \sum_{F_\ell' F_\ell} \sum_{F_u' F_u} \sqrt{2F_\ell' + 1} \Upsilon(L_u L_\ell S I, J_u J_u' J_\ell J_\ell' F_u F_u' F_\ell F_\ell') \\
&\times \frac{1}{2} \left[\frac{\Phi(\nu_{J_u F_u, J_\ell F_\ell} - \nu) + \Phi(\nu_{J_u' F_u', J_\ell' F_\ell'} - \nu)^*}{1 + \epsilon' + 2\pi i \nu J_u' F_u' / A(L_u \rightarrow L_\ell)} \right] \epsilon' \\
&\times \sum_K (-1)^{F_u - F_u' - F_\ell + F_\ell' + K} \sqrt{3} \begin{Bmatrix} K & F_u & F_u' \\ F_\ell & 1 & 1 \end{Bmatrix} \begin{Bmatrix} F_u' & F_\ell' & 1 \\ F_\ell' & F_u & K \end{Bmatrix} \sigma_0^K(J_\ell', F_\ell'). \quad (31)
\end{aligned}$$

Also in this case, we verified that if lower term polarization is neglected and in the absence of HFS, Eq. (30) reduces to Eq. (29) of Belluzzi & Trujillo Bueno (2014).

5. The radiative transfer equations

We consider a plane-parallel atmosphere in the absence of magnetic fields. The problem is thus characterized by cylindrical symmetry along the direction perpendicular to the surface of the atmosphere (hereafter, the “vertical”). Taking the quantization axis directed along the vertical, and the reference direction for positive Q parallel to the surface, at any height in the atmosphere the radiation field is described by the Stokes parameters I and Q only (hereafter always indicated as I_0 and I_1 , respectively), while J_0^0 and J_0^2 are the only non-vanishing elements of the radiation field tensor. Under the above-mentioned hypotheses, and neglecting stimulated emission, the RT equation takes the form

$$\frac{d}{ds} \begin{pmatrix} I_0(\nu, \vec{\Omega}) \\ I_1(\nu, \vec{\Omega}) \end{pmatrix} = - \begin{pmatrix} \eta_0(\nu, \vec{\Omega}) & \eta_1(\nu, \vec{\Omega}) \\ \eta_1(\nu, \vec{\Omega}) & \eta_0(\nu, \vec{\Omega}) \end{pmatrix} \begin{pmatrix} I_0(\nu, \vec{\Omega}) \\ I_1(\nu, \vec{\Omega}) \end{pmatrix} + \begin{pmatrix} \varepsilon_0(\nu, \vec{\Omega}) \\ \varepsilon_1(\nu, \vec{\Omega}) \end{pmatrix}, \quad (32)$$

where s is the spatial coordinate measured along the ray path. The emission and absorption coefficients appearing in Eq. (32) contain both the line and the continuum contributions (hereafter indicated with the apices ℓ and c , respectively):

$$\eta_i(\nu, \vec{\Omega}) = \eta_i^\ell(\nu, \vec{\Omega}) + \eta_i^c(\nu, \vec{\Omega}) , \quad (33)$$

$$\varepsilon_i(\nu, \vec{\Omega}) = \varepsilon_i^\ell(\nu, \vec{\Omega}) + \varepsilon_i^c(\nu, \vec{\Omega}) . \quad (34)$$

The line absorption coefficient, $\eta_i^\ell(\nu, \vec{\Omega})$, is given by Eq. (11). Using Eqs. (20), (28), and (30), the line emission coefficient, $\varepsilon_i^\ell(\nu, \vec{\Omega})$, can be written in the form

$$\varepsilon_i^\ell(\nu, \vec{\Omega}) = k_L \sum_{KQ} \mathcal{T}_Q^K(i, \vec{\Omega}) \left(\tilde{J}_Q^K(\nu) + \delta_{Q0} B_T(\nu_0) \beta_0^K(\nu) \right) , \quad (35)$$

with

$$\tilde{J}_Q^K(\nu) = \sum_{K_r Q_r} \int d\nu' J_{Q_r}^{K_r}(\nu') r_{II-AA}(KQ, K_r Q_r; \nu', \nu) . \quad (36)$$

We consider the contribution of a coherent polarized continuum. Neglecting dichroism (which is a very good approximation in the visible part of the solar spectrum), the continuum total absorption coefficient (opacity) is given by

$$\eta_i^c(\nu) = [k_c(\nu) + \sigma(\nu)] \delta_{i0} , \quad (37)$$

with $k_c(\nu)$ the continuum true absorption coefficient, and $\sigma(\nu)$ the continuum scattering coefficient. The continuum emission coefficient is given by

$$\varepsilon_i^c(\nu, \vec{\Omega}) = \sigma(\nu) \sum_{KQ} \mathcal{T}_Q^K(i, \vec{\Omega}) (-1)^Q J_{-Q}^K(\nu) + \varepsilon_{\text{th}}^c(\nu) \delta_{i0} . \quad (38)$$

The first term in the right-hand side of Eq. (38) represents the contribution to the continuum emission coefficient coming from coherent scattering processes (Rayleigh and Thomson scattering), the second term represents the thermal contribution (which does not contribute to the polarization of the continuum). Under the assumption that the continuum is in LTE, $\varepsilon_{\text{th}}^c(\nu) = k_c(\nu) B_T(\nu)$.

As is clear from Eq. (32), when dichroism is taken into account (i.e., when η_1 is non-zero), the RT equations for the Stokes parameters I_0 and I_1 are coupled to each other. However, they can be easily decoupled by introducing the quantities

$$\begin{aligned} \hat{I}_0(\nu, \vec{\Omega}) &= I_0(\nu, \vec{\Omega}) + I_1(\nu, \vec{\Omega}) , \\ \hat{I}_1(\nu, \vec{\Omega}) &= I_0(\nu, \vec{\Omega}) - I_1(\nu, \vec{\Omega}) . \end{aligned} \quad (39)$$

Indeed, from Eqs. (32) and (39), it can be easily shown that the RT equations for $\hat{I}_j(\nu, \vec{\Omega})$ ($j = 0, 1$) are given by

$$\frac{d}{ds} \hat{I}_j(\nu, \vec{\Omega}) = -\hat{\eta}_j(\nu, \vec{\Omega}) \hat{I}_j(\nu, \vec{\Omega}) + \hat{\varepsilon}_j(\nu, \vec{\Omega}) , \quad (40)$$

with

$$\hat{\varepsilon}_j(\nu, \vec{\Omega}) = \varepsilon_0(\nu, \vec{\Omega}) + (-1)^j \varepsilon_1(\nu, \vec{\Omega}) , \quad (41)$$

$$\hat{\eta}_j(\nu, \vec{\Omega}) = \eta_0(\nu, \vec{\Omega}) + (-1)^j \eta_1(\nu, \vec{\Omega}) . \quad (42)$$

The Stokes parameters I_0 and I_1 can be easily obtained from the new quantities through the relations

$$\begin{aligned} I_0(\nu, \vec{\Omega}) &= \frac{1}{2} \left(\hat{I}_0(\nu, \vec{\Omega}) + \hat{I}_1(\nu, \vec{\Omega}) \right) , \\ I_1(\nu, \vec{\Omega}) &= \frac{1}{2} \left(\hat{I}_0(\nu, \vec{\Omega}) - \hat{I}_1(\nu, \vec{\Omega}) \right) . \end{aligned} \quad (43)$$

It can be easily shown that the quantities $\hat{\eta}_j^\ell(\nu, \vec{\Omega})$, and $\hat{\varepsilon}_j^\ell(\nu, \vec{\Omega})$ are given by Eqs. (11) and (35), respectively, provided that the geometrical tensor $\mathcal{T}_Q^K(i, \vec{\Omega})$ appearing in such equations is substituted by

$$\hat{\mathcal{T}}_Q^K(j, \vec{\Omega}) = \mathcal{T}_Q^K(0, \vec{\Omega}) + (-1)^j \mathcal{T}_Q^K(1, \vec{\Omega}) \quad j = 0, 1 . \quad (44)$$

On the other hand, we have

$$\hat{\eta}_j^c(\nu) = \eta_0^c(\nu) = k_c(\nu) + \sigma(\nu) \quad j = 0, 1 , \quad (45)$$

and

$$\hat{\varepsilon}_j^c(\nu, \vec{\Omega}) = \sigma(\nu) \sum_{KQ} \hat{\mathcal{T}}_Q^K(j, \vec{\Omega}) (-1)^Q J_{-Q}^K(\nu) + \varepsilon_{\text{th}}^c(\nu) \quad j = 0, 1 . \quad (46)$$

In terms of the new quantities $\hat{I}_j(\nu, \vec{\Omega})$ and $\hat{\mathcal{T}}_Q^K(j, \vec{\Omega})$, the radiation field tensor is given by

$$J_Q^K(\nu) = \int \frac{d\Omega}{4\pi} \sum_{j=0}^1 \mathcal{T}_Q^K(j, \vec{\Omega}) I_j(\nu, \vec{\Omega}) = \frac{1}{2} \int \frac{d\Omega}{4\pi} \sum_{j=0}^1 \hat{\mathcal{T}}_Q^K(j, \vec{\Omega}) \hat{I}_j(\nu, \vec{\Omega}) . \quad (47)$$

Introducing the optical depth $\hat{\tau}_j(\nu, \vec{\Omega})$ defined by

$$d\hat{\tau}_j(\nu, \vec{\Omega}) = -\hat{\eta}_j(\nu, \vec{\Omega}) ds , \quad (48)$$

and the source function

$$\hat{S}_j(\nu, \vec{\Omega}) = \frac{\hat{\varepsilon}_j(\nu, \vec{\Omega})}{\hat{\eta}_j(\nu, \vec{\Omega})} , \quad (49)$$

the RT equation for the quantities \hat{I}_j takes the form

$$\frac{d}{d\hat{\tau}_j(\nu, \vec{\Omega})} \hat{I}_j(\nu, \vec{\Omega}) = \hat{I}_j(\nu, \vec{\Omega}) - \hat{S}_j(\nu, \vec{\Omega}) . \quad (50)$$

The source function $\hat{S}_j(\nu, \vec{\Omega})$ can be conveniently written in the form

$$\hat{S}_j(\nu, \vec{\Omega}) = \frac{k_L}{\hat{\eta}_j(\nu, \vec{\Omega})} \sum_{KQ} \hat{\mathcal{T}}_Q^K(j, \vec{\Omega}) S_Q^K(\nu) , \quad (51)$$

with

$$S_Q^K(\nu) = \check{J}_Q^K(\nu) + \delta_{Q0} B_T(\nu_0) \beta_0^K(\nu) + \delta_{K0} \delta_{Q0} \frac{\varepsilon_{\text{th}}^c(\nu)}{k_L} . \quad (52)$$

The quantity $\check{J}_Q^K(\nu)$ is given by

$$\check{J}_Q^K(\nu) = \tilde{J}_Q^K(\nu) + s(\nu) (-1)^Q J_{-Q}^K(\nu) = \sum_{K_r Q_r} \int d\nu' J_{Q_r}^{K_r}(\nu') \psi_{KQ, K_r Q_r}(\nu', \nu) , \quad (53)$$

with $s(\nu) = \sigma(\nu)/k_L$, and

$$\psi_{KQ, K_r Q_r}(\nu', \nu) = \left[r_{II-AA}(KQ, K_r Q_r; \nu', \nu) + \delta_{K_r K} \delta_{Q_r -Q} \delta(\nu - \nu') s(\nu) (-1)^Q \right] . \quad (54)$$

6. Iterative solution of the non-LTE problem

The calculation of $J_0^0(\nu)$ and $J_0^2(\nu)$ at each height in the atmosphere requires the knowledge of the quantities $\hat{I}_j(\nu, \vec{\Omega})$ along the various directions of the chosen angular quadrature, as obtained from the solution of Eq. (50). The formal solution of this equation is given by

$$\hat{I}_j(\nu, \mu; O) = \hat{I}_j(\nu, \mu; M) e^{-\Delta \hat{\tau}_j(\nu, \mu)} + \int_0^{\Delta \hat{\tau}_j(\nu, \mu)} \hat{S}_j(\nu, \mu; t) e^{-t} dt , \quad (55)$$

where O is a given height point in the considered discretization of the atmosphere, and M is the corresponding “upwind” point. As far as the dependence on the propagation direction is concerned, we have taken into account that, due to the cylindrical symmetry of the problem, the various quantities only depend on $\mu = \cos \theta$, with θ the angle between the vertical and the propagation direction. The quantity $\Delta \hat{\tau}_j(\nu, \mu)$ is the optical distance between O and M , at frequency ν , along the direction specified by μ . We evaluate the integral in the right-hand side of Eq. (55) by means of the short-characteristic method (see Kunasz & Auer 1988). Indicating the values of \hat{I}_j and \hat{S}_j at the various points of the spatial grid through the elements of column vectors, the formal solution of the RT equation can be written in the form

$$\hat{I}_j(\nu, \mu; \ell) = \sum_{m=1}^N \Lambda_{\nu\mu}^j(\ell, m) \hat{S}_j(\nu, \mu; m) + \hat{T}_j(\nu, \mu; \ell) , \quad (56)$$

where $\ell, m = 1, \dots, N$, with N number of grid points, $\hat{T}_j(\nu, \mu; \ell)$ is the value of the transmitted $\hat{I}_j(\nu, \mu)$ at point ℓ due to the radiation incident at the boundary, and $\Lambda_{\nu\mu}^j(\ell, m)$ are the elements of a $N \times N$ operator.

Substituting Eq. (56) into Eq. (47) the operations required for the numerical calculation of $J_0^K(\nu)$ at point ℓ can be indicated as follows:

$$J_0^K(\nu; \ell) = \sum_{m=1}^N \sum_{K'} \Lambda_{K0, K'0}(\nu; \ell, m) S_0^{K'}(\nu; m) + T_0^K(\nu; \ell) , \quad (57)$$

where we have explicitly indicated the dependence on the height point in the atmosphere of the various physical quantities previously introduced. The Λ operators and the T_0^K tensor are given by

$$\Lambda_{K0,K'0}(\nu; \ell, m) = \frac{1}{2} \int \frac{d\vec{\Omega}}{4\pi} \sum_{j=0}^1 \Lambda_{\nu\mu}^j(\ell, m) \frac{k_L(m)}{\hat{\eta}_j(\nu, \mu; m)} \hat{\mathcal{T}}_0^K(j, \vec{\Omega}) \hat{\mathcal{T}}_0^{K'}(j, \vec{\Omega}) , \quad (58)$$

$$T_0^K(\nu; \ell) = \frac{1}{2} \int \frac{d\vec{\Omega}}{4\pi} \sum_{j=0}^1 \hat{\mathcal{T}}_0^K(j, \vec{\Omega}) \hat{T}_j(\nu, \mu; \ell) . \quad (59)$$

The equations for S_0^0 and S_0^2 resulting from the substitution of Eq. (57) into Eq. (52) (through Eq. (53)) represent the fundamental equations for the non-LTE problem under consideration. It is well known that the most suitable approach for the numerical solution of this set of equations is through iterative methods. In this work, we apply the Jacobian-based iterative method.

Let $S_0^{0\text{old}}$ and $S_0^{2\text{old}}$ be given estimates of the unknowns at the various points of the grid. At any grid point ℓ , we calculate J_0^0 and J_0^2 through Eq. (57) by using such “old” values of the source function at all the grid points, except at point ℓ where the new estimates, $S_0^{0\text{new}}$ and $S_0^{2\text{new}}$, are *implicitly* (their value being still unknown) used:

$$J_0^K(\nu; \ell) = J_0^K(\nu; \ell)^{\text{old}} + \sum_{K'} \Lambda_{K0,K'0}(\nu; \ell, \ell) \Delta S_0^{K'}(\nu; \ell) , \quad (60)$$

with

$$\Delta S_0^{K'}(\nu; \ell) = S_0^{K'}(\nu; \ell)^{\text{new}} - S_0^{K'}(\nu; \ell)^{\text{old}} , \quad (61)$$

and where $J_0^0(\nu; \ell)^{\text{old}}$ and $J_0^2(\nu; \ell)^{\text{old}}$ are the values of J_0^0 and J_0^2 that are obtained from a formal solution of the RT equation, carried out using the “old” estimates $S_0^{0\text{old}}$ and $S_0^{2\text{old}}$. The following step is to calculate $\check{J}_0^K(\nu; \ell)$ through Eq. (53):

$$\check{J}_0^K(\nu; \ell) = \check{J}_0^K(\nu; \ell)^{\text{old}} + \sum_{K_r K_r'} \int d\nu' \psi_{K0, K_r 0}(\nu', \nu; \ell) \Lambda_{K_r 0, K_r' 0}(\nu'; \ell, \ell) \Delta S_0^{K_r'}(\nu'; \ell) . \quad (62)$$

The new values of the source function are finally obtained by substituting Eq. (62) into Eq. (52):

$$\Delta S_0^K(\nu; \ell) = \sum_{K_r K_r'} \int d\nu' \psi_{K0, K_r 0}(\nu', \nu; \ell) \Lambda_{K_r 0, K_r' 0}(\nu'; \ell, \ell) \Delta S_0^{K_r'}(\nu'; \ell) + R_0^K(\nu, \ell) , \quad (63)$$

with

$$R_0^K(\nu; \ell) = \check{J}_0^K(\nu; \ell)^{\text{old}} + B_T(\nu_0; \ell) \beta_0^K(\nu; \ell) + \delta_{K0} \frac{\varepsilon_{\text{th}}^c(\nu; \ell)}{k_L(\ell)} - S_0^K(\nu; \ell)^{\text{old}} . \quad (64)$$

The Jacobi-based method that we apply in this work is obtained by setting $\Lambda_{K0, K'0} = \Lambda_{00, 00} \delta_{K0} \delta_{K'0}$ (see Trujillo Bueno & Manso Sainz 1999, for a detailed discussion on the role of the various Λ -operators). Introducing the ensuing expressions into Eq. (52) we obtain

$$\Delta S_0^0(\nu; \ell) = \int d\nu' \psi_{00, 00}(\nu', \nu; \ell) \Lambda_{00, 00}(\nu'; \ell, \ell) \Delta S_0^0(\nu'; \ell) + R_0^0(\nu; \ell) , \quad (65)$$

$$\Delta S_0^2(\nu; \ell) = \int d\nu' \psi_{20,00}(\nu', \nu; \ell) \Lambda_{00,00}(\nu'; \ell, \ell) \Delta S_0^0(\nu'; \ell) + R_0^2(\nu; \ell). \quad (66)$$

We calculate the new estimate of S_0^0 by solving Eq. (65) through the so-called “Frequency-by-frequency” method.

7. Results

In this section, we present and discuss the scattering polarization profiles of the Na I D₁ line resulting from the numerical solution of the non-LTE problem described in the previous sections, in two semi-empirical models of the solar atmosphere. In particular, we show how the Q/I signal produced in the core of the D₁ line by the mechanism pointed out by Belluzzi & Trujillo Bueno (2013) is affected by quantum interference between the upper J -levels of D₁ and D₂, and by the presence of an increasing amount of atomic polarization in the ground level of sodium. Although our work is focused on the D₁ line, we present and discuss also the polarization profiles of the D₂ line, which is naturally included in our calculations.

7.1. Sensitivity to the atmospheric model (No Lower Level Polarization)

Figure 1 shows the Q/I profiles calculated in model C of Fontenla et al. (1993) (hereafter, FAL-C), and in model M_{CO} (also known as FAL-X) of Avrett (1995), assuming that there is no atomic polarization in the lower levels. As far as the D₂ line is concerned, the theoretical profile shows the typical triplet peak structure that is observed in this line. The central peak of the calculated profile has a small but appreciable sub-structure, which is sensibly reduced once the I and Q profiles are convolved with a gaussian, so to take the spectral smearing due to the finite bandwidth of the instrument into account. While in the observed profiles the central peak is higher than the wing peaks, in our theoretical profile the three peaks have approximately the same amplitude. Although the presence of lower level polarization produces an increase of the amplitude of the central peak (see Sect. 7.2), we believe that the main reason for this disagreement with the observations has to be sought in the assumption of purely coherent scattering in the atom rest frame. Indeed, calculations carried out within the framework of the PRD approach of Bommier (1997), considering a simpler two-level model atom, show that the R_{II} part of the redistribution matrix, which describes the contribution of scattering processes in the limit of CRD, produces a decrease of the amplitude of the wing peaks, leaving almost unaffected the central one. This is not surprising since the central peak forms much higher in the atmosphere, where the impact of collisions capable of redistributing the photon frequency during the scattering process is negligible. We finally observe that the two peaks in the wings of the line do not have the same amplitude, the red one being slightly smaller than the blue one. This is due to the effect of J -state interference, and it is in agreement with the observed profiles.

Moving toward longer wavelengths, the theoretical profile reproduces the sign reversal that is observed between D₁ and D₂ very well, as well as the general pattern that is observed in the wings of the D₁ line. We recall that these are the typical signatures of J -state interference (see Stenflo 1980;

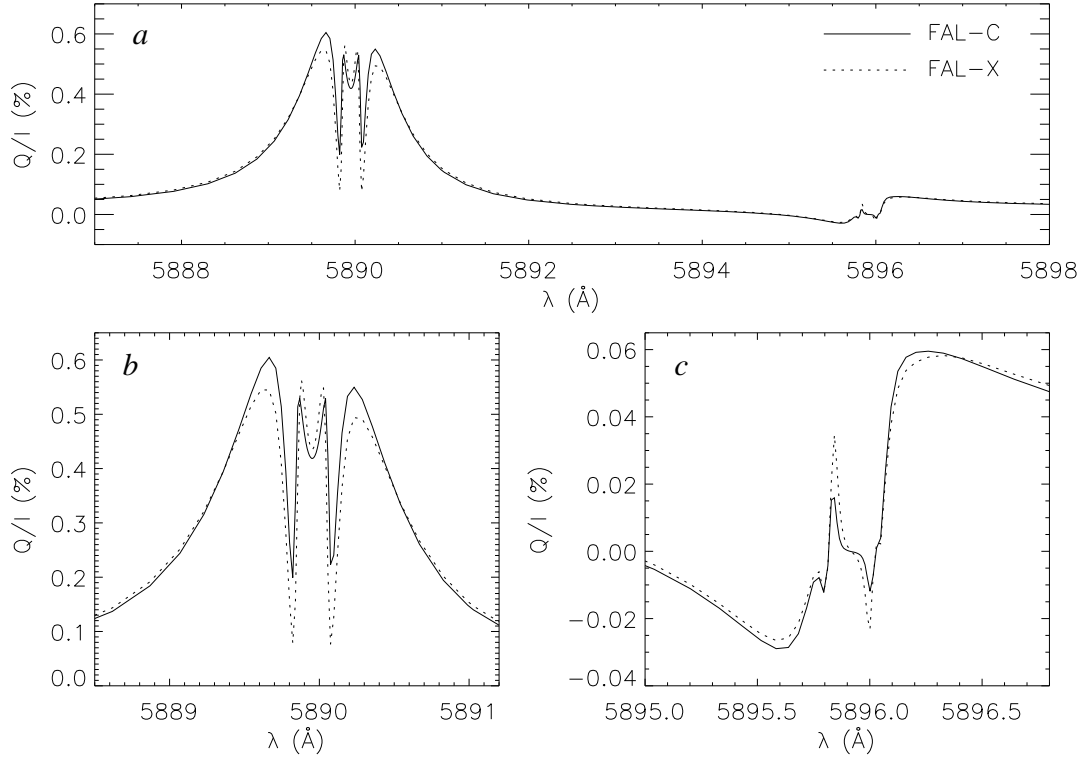


Fig. 1.— Fractional linear polarization profiles calculated in the FAL-C (solid) and FAL-X (dotted) atmospheric models, for a line of sight with $\mu = 0.1$ (μ being the cosine of the heliocentric angle), in the absence of lower level polarization. The reference direction for positive Q is parallel to the solar limb. *Panel a:* spectral interval containing both D₁ and D₂. *Panel b:* zoom on the D₂ line. *Panel c:* zoom on the D₁ line.

Landi Degl’Innocenti & Landolfi 2004; Belluzzi & Trujillo Bueno 2011), which are fully accounted for in our theoretical approach. In the core of the D₁ line, we obtain a clear Q/I signal, with positive and negative peaks leading to an almost null integrated polarization signal. The positive peak is slightly blue-shifted with respect to line center (where the signal is zero), while the negative one is slightly red-shifted. A small negative dip can also be recognized between the positive peak and the negative minimum of the J -state interference pattern. Remarkably, this signal is not due either to lower level polarization or to the presence of a magnetic field (both ingredients have been neglected in the calculations of Fig. 1), but it is produced by the physical mechanism identified and discussed by Belluzzi & Trujillo Bueno (2013). It is important to note that this signal appears in the core of the D₁ line, where the assumption of purely coherent scattering in the atom rest frame is a good approximation and the contribution of R_{III} (not included in this work) can be safely neglected. The amplitude of the positive and negative peaks is quite sensitive to the atmospheric model. In particular, in agreement with the results of Belluzzi & Trujillo Bueno (2013), the peaks obtained in FAL-X are almost two times larger than those calculated in FAL-C. Nonetheless, the amplitude of our theoretical profiles remains sensibly smaller than that of the signal observed by Stenflo & Keller (1997), although it is in agreement with other observations (e.g., Trujillo Bueno et al. 2001).

The presence of non-zero signals in the core of the Na I D₁ line has been confirmed by recent observations carried out with the Zürich Imaging Polarimeter (ZIMPOL) at the Istituto Ricerche Solari Locarno (such observations will be published in a forthcoming paper). These signals, which show conspicuous variations along the slit, are much more similar to our theoretical profiles than to the large signal observed by Stenflo & Keller (1997). As it will be shown below, the presence of ad-hoc amounts of atomic polarization in the ground level of sodium allows us to significantly increase the amplitude of our theoretical profiles. On the other hand, the physical mechanism pointed out by Belluzzi & Trujillo Bueno (2013), possibly together with the presence of some lower level polarization, appears to be perfectly suitable for explaining the Q/I signals revealed by the recent observations.

7.2. The impact of lower level polarization

We include now a given amount of atomic polarization in the lower F -levels, parametrizing the quantity σ_0^2 defined in Eq. (7) according to the following expression

$$\sigma_0^2(F_\ell, h) = \frac{a(F_\ell)}{1 + b(F_\ell) \tau_{v_0}(h)} , \quad (67)$$

where h is the geometrical height in the atmosphere, and τ_{v_0} is the optical depth along the vertical, at the line center frequency of the D₂ line. The parameter a represents the value of σ_0^2 at the top of the atmosphere, while b sets its scale height. A similar parametrization of lower level polarization was used by Landi Degl’Innocenti (1998).

Figure 2 shows the Q/I profiles of the D₁ and D₂ lines calculated in the FAL-X model, for different values of the parameter $b(F_\ell)$, keeping fixed the parameter $a(F_\ell)$. We set $b(F_\ell = 1) = b(F_\ell = 2)$, and $a(F_\ell = 2) = 2a(F_\ell = 1)$ (we recall that a ratio of about 2 between the atomic polarization of the levels

$F_\ell = 2$ and $F_\ell = 1$ was also considered by Landi Degl’Innocenti 1998, in order to obtain his best fit to the observed profiles). In the D_2 line, lower level polarization produces an appreciable increase of the amplitude of the central peak, and a slight modification of its sub-structure. On the other hand, the two peaks in the wings, as well as the dips between the central and wing peaks are unchanged. As expected, the increase of the central peak is larger for smaller values of the parameter b , that is, when the value of σ_0^2 starts decreasing below the height of formation of the line.

Also in the D_1 line, the presence of atomic polarization in the lower F -levels produces an increase of the amplitude of the Q/I signal. Although both the positive and negative peaks are increased, the variation is sensibly larger in the negative one. Interestingly, the small negative structure in the blue wing is not affected by lower level polarization. Contrary to the D_2 line, the impact of lower level polarization is almost negligible for $b = 10$, while for $b = 0.1$, the profile starts being very similar to the one calculated by Landi Degl’Innocenti (1998).

Figure 3 shows the Q/I profiles of the D_1 and D_2 lines calculated in the FAL-X model, for different values of the parameter $a(F_\ell = 2)$, assuming $a(F_\ell = 1) = 0.01$ and $b(F_\ell = 1) = b(F_\ell = 2) = 0.1$. The amplitudes of the central peak of D_2 , and of the positive and negative peaks of the Q/I signal of D_1 increase proportionally to the atomic polarization of the lower level $F_\ell = 2$. As in the previous case, the variation of the signal amplitude in the D_1 line is larger in the negative peak than in the positive one. Interestingly, the sub-structure of the central peak of D_2 becomes more asymmetric when increasingly different amounts of atomic polarization in the lower levels $F_\ell = 1$ and $F_\ell = 2$ are considered.

7.3. Center-to-limb variation

Moving from the limb to disk center, the amplitude of the central peak and of the wing peaks of the D_2 line Q/I profile gradually decreases (see left panel of Fig. 4). The value of the two dips between the central peak and the wing peaks changes from positive to negative while going from $\mu = 0.1$ to $\mu = 0.2$. It reaches a (negative) minimum around $\mu = 0.4$, and it finally starts decreasing (in absolute value), going to zero, for larger values of μ . The figure shows the Q/I profiles up to $\mu = 0.6$. For larger μ -values the whole profile goes gradually to zero without changing its shape and sign.

As far as the D_1 line is concerned, it can be observed that the amplitude of both the positive and negative peaks gradually decreases going from the limb to disk center (see right panel of Fig. 4). The small negative dip in the blue wing of the line remains almost unchanged going from $\mu = 0.1$ to $\mu = 0.4$, and only for higher values of μ its amplitude starts decreasing. Interestingly, in the red wing of the line, where, for $\mu = 0.1$, a small and almost flat positive feature is obtained, going to $\mu = 0.2$ we find another small, but appreciable, negative dip. This dip does not change appreciably going from $\mu = 0.2$ to $\mu = 0.6$. As for the case of the D_2 line, for values of μ larger than 0.6 (not shown in the figure), the whole Q/I profile of the D_1 line goes gradually to zero without changing its shape and sign.

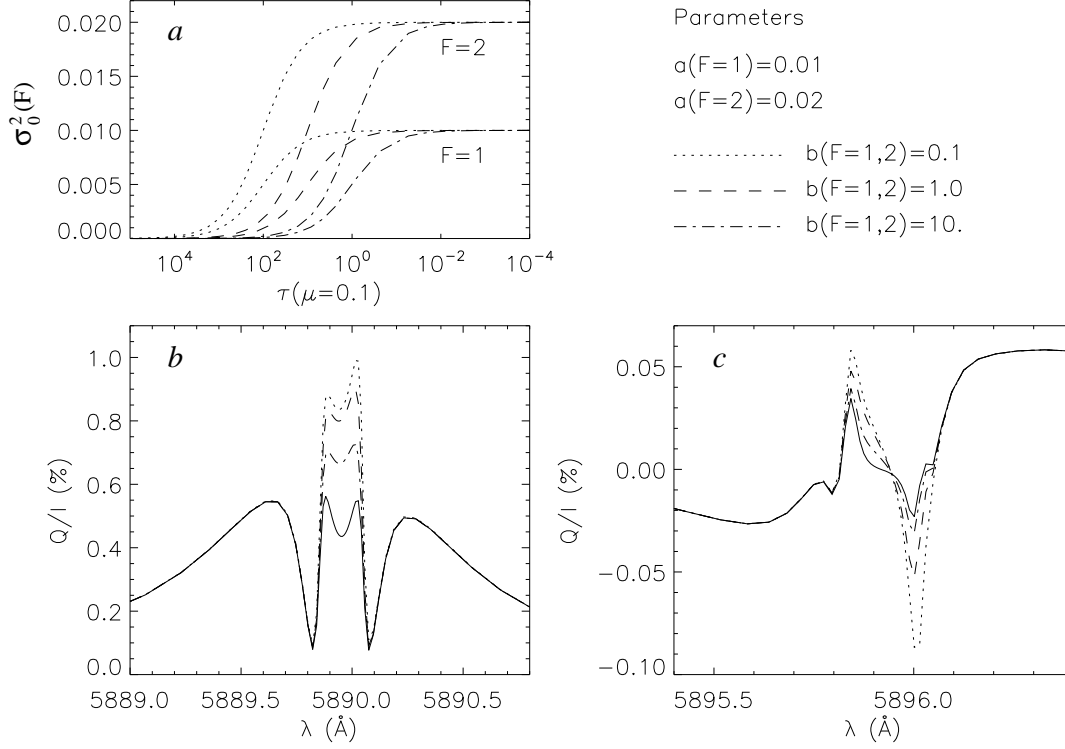


Fig. 2.— *Panel a*: plot of $\sigma_0^2(F_\ell = 2)$ (upper lines) and $\sigma_0^2(F_\ell = 1)$ (lower lines) as a function of the optical depth, τ , measured along the line of sight ($\mu = 0.1$), at the line center frequency of the D₂ line, in the FAL-X model, for three different values of the parameter b . The values of the parameters a and b in the three cases considered are indicated in the figure. *Panel b*: fractional linear polarization profiles of the D₂ line, calculated for the three different parametrizations of lower level polarization shown in panel *a*. The profile with the solid line corresponds to the case of no lower level polarization (it coincides with the dotted profile in panel *b* of Fig. 1), and it is included for reference. All of the profiles have been calculated in the FAL-X model, for $\mu = 0.1$. *Panel c*: same as panel *b*, but for the D₁ line.

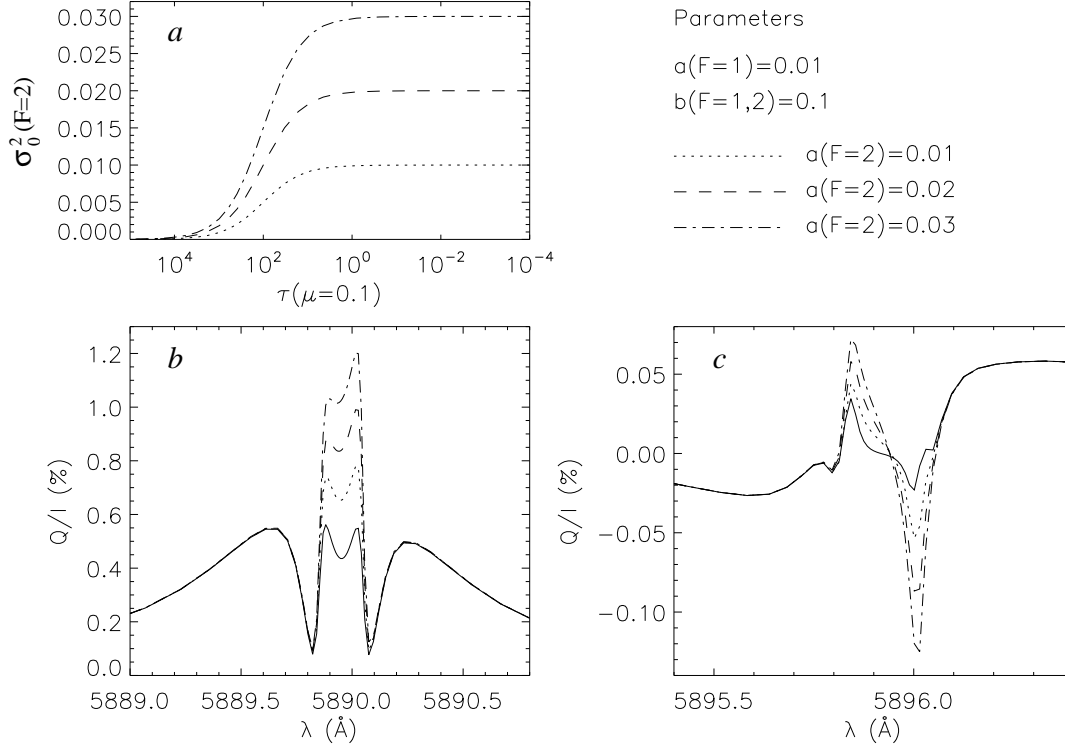


Fig. 3.— *Panel a*: plot of $\sigma_0^2(F_\ell = 2)$ as a function of optical depth (along the line-of-sight, at the line center frequency of D_2) in the FAL-X model, for three different values of the parameter $a(F_\ell = 2)$. The values of the parameters a and b in the three cases considered are indicated in the figure. *Panel b*: fractional linear polarization profiles of the D_2 line, calculated for the three different parametrizations of lower level polarization shown in panel *a*. The profile with the solid line corresponds to the case of no lower level polarization (it coincides with the dotted profile in panel *b* of Fig. 1), and it is included for reference. All of the profiles have been calculated in the FAL-X model, for $\mu = 0.1$. *Panel c*: same as panel *b*, but for the D_1 line.

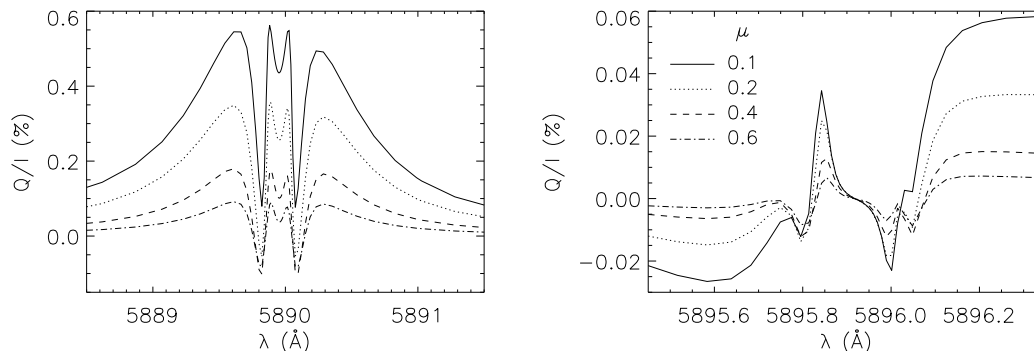


Fig. 4.— *Left panel:* center-to-limb variation of the D₂ line Q/I profile calculated in the FAL-X atmospheric model, in the absence of atomic polarization in the lower level. The values of μ corresponding to the various profiles are indicated in the right panel. *Right panel:* same as left panel, but for the D₁ line.

8. Concluding comments

The modeling of the linear polarization produced by resonance scattering in the solar atmosphere is a complex radiative transfer problem, especially when strong spectral lines resulting from HFS multiplets are considered. This is because there are, in general, several mechanisms and physical ingredients that need to be taken into account for explaining the observed spectral line polarization: frequency correlations between the incoming and outgoing photons along with the spectral structure of the incident radiation field, ground-level polarization, and quantum interference among FS and HFS levels. In this work, we have developed a theoretical and numerical approach suitable for solving the non-LTE radiative transfer problem for polarized radiation, taking the above-mentioned ingredients into account.

The theoretical approach is based on the density-matrix multilevel theory proposed by Landi Degl’Innocenti et al. (1997), according to which each atomic level is considered as a continuous distribution of sublevels. We consider a two-term atomic model with HFS, with prescribed atomic polarization in the F -levels of the ground level, and we focus on the limit of coherent scattering in the atomic rest frame, taking into account the effects of Doppler redistribution in the observer’s frame. Moreover, in addition to the radiative transitions we include excitations and de-excitations due to inelastic collisions with electrons, as explained in Belluzzi et al. (2015). As far as elastic collisions with neutral hydrogen atoms are concerned, in this first step, we have neglected them, except for their line broadening effect (see footnote 2). With these assumptions, radiative transfer applications aimed at modeling the fractional scattering polarization observed in strong resonance lines are expected to be appropriate concerning the core of the lines. The numerical approach is a careful generalization of the methods explained in Belluzzi & Trujillo Bueno (2014).

A detailed application to the D-lines of Na I, with emphasis on the enigmatic D₁ line, has allowed us to analyze the observable signatures of all the above-mentioned physical mechanisms. In agreement with Belluzzi & Trujillo Bueno (2013), we conclude that the enigmatic linear polarization observed in the core

of the sodium D₁ line may be explained by the effect that one gets when taking properly into account the detailed spectral structure of the incident solar D₁-line radiation over the small frequency interval spanned by the HFS transitions. Interestingly, this key mechanism is capable of introducing significant scattering polarization in the core of the Na I D₁ line without the need for ground-level polarization.

IRSOL gratefully acknowledges financial support from the Swiss State Secretariat for Education, Research and Innovation (SERI), Canton Ticino, the city of Locarno, local municipalities, Aldo e Cele Daccò foundation, and the Swiss National Science Foundation through grant 200020-157103 (Astrophysical Spectropolarimetry). Financial support by the Spanish Ministry of Economy and Competitiveness through projects AYA2010-18029 (Solar Magnetism and Astrophysical Spectropolarimetry) and AYA2014-60476-P is also gratefully acknowledged.

REFERENCES

- Avrett, E.H. 1995, in *Infrared Tools for Solar Astrophysics: What's Next?*, eds. J.R. Kuhn & M.J. Penn (Singapore: World Scientific), 303
- Belluzzi, L., & Trujillo Bueno, J. 2011, *ApJ*, 743, 3
- Belluzzi, L., & Trujillo Bueno, J. 2013, *ApJ*, 774, 28L
- Belluzzi, L., & Trujillo Bueno, J. 2014, *A&A*, 564, 16
- Belluzzi, L., Landi Degl'Innocenti, E., & Trujillo Bueno, J. 2015, *ApJ*, 812, 73
- Bianda, M., Solanki, S.K., & Stenflo, J.O. 1998, *A&A*, 331, 760
- Bommier, V. 1997, *A&A*, 328, 706
- Casini, R., Landi Degl'Innocenti, E., Landolfi, M., & Trujillo Bueno, J. 2002, *ApJ*, 573, 864
- Casini, R., & Manso Sainz, R. 2005, *ApJ*, 624, 1025
- Del Pino Alemán, T., Manso Sainz, R., & Trujillo Bueno, J. 2014, *ApJ*, 784, 46
- Fontenla, J.M., Avrett, E.H., & Loeser, R. 1993, *ApJ*, 406, 319
- Hummer, D.G. 1962, *MNRAS*, 125, 21
- Kerkeni, B., & Bommier, V. 2002, *A&A*, 394, 707
- Kunasz, P., & Auer, L.H. 1988, *J. Quant. Spec. Radiat. Transf.*, 39, 67
- Landi Degl'Innocenti, E. 1983, *Sol. Phys.*, 85, 3
- Landi Degl'Innocenti, E. 1998, *Nature*, 392, 256

- Landi Degl’Innocenti, E. 1999, in *Solar Polarization*, eds. K.N. Nagendra and J.O. Stenflo, ASSL 243, 61
- Landi Degl’Innocenti, E., & Landolfi, M. 2004, *Polarization in Spectral Lines* (Dordrecht: Kluwer)
- Landi Degl’Innocenti, E., Landi Degl’Innocenti, M., & Landolfi, M. 1997, in *Science with THÉMIS*, eds. N. Mein, and S. Sahal-Bréchet (Paris: Obs. Paris-Meudon), 59
- Rees, D.E., & Saliba G.J. 1982, *A&A*, 115, 1
- Stenflo, J.O. 1980, *A&A*, 84, 68
- Stenflo, J.O., & Keller, C.U. 1997, *A&A*, 321, 927
- Stenflo, J.O, Keller, C.U., & Gandorfer, A. 1998, *A&A*, 329, 319
- Stenflo, J.O, Keller, C.U., & Gandorfer, A. 2000, *A&A*, 355, 789
- Stenflo, J.O. 2015, *ApJ*, 801, 70
- Thalmann, C., Stenflo, J.O., Feller, A., & Cacciani, A. 2006, in *Solar Polarization 4*, eds. R. Casini & B. Lites, ASP Conf. Ser. 358, 323
- Thalmann, C., Stenflo, J.O., Feller, A., & Cacciani, A. 2009, in *Solar Polarization 5*, eds. S.V. Berdyugina, K.N. Nagendra, & R. Ramelli, ASP Conf. Ser. 405, 113
- Trujillo Bueno, J. 2009, in *Solar Polarization 5*, eds. S.V. Berdyugina, K.N. Nagendra, & R. Ramelli, ASP Conf. Ser. Vol. 405, 65
- Trujillo Bueno, J. & Manso Sainz, R. 1999, *ApJ*, 516, 436
- Trujillo Bueno, J., Collados, M., Paletou, F., & Molodij, G. 2001, in *Advanced Solar Polarimetry — Theory, Observations, and Instrumentation*, ed. M. Sigwarth, ASP Conf. Ser. Vol. 236, 141
- Trujillo Bueno, J., Casini, R., Landolfi, M., & Landi Degl’Innocenti, E. 2002, *ApJ*, 566, 53